Proceedings of ASME Turbo Expo 2011
GT2011
June 6-10, 2011, Vancouver, British Columbia, Canada

GT2011-46621

COMPRESSOR BLADE MODELLING UNDER HIGHLY NEGATIVE INCIDENCE

Pavlos K. Zachos, Cornelia Ruelke, Vassilios Pachidis, Riti Singh
Department of Power and Propulsion
School of Engineering
Cranfield University, MK43 0AL, UK
Email: p.zachos@cranfield.ac.uk

ABSTRACT

This paper investigates performance prediction techniques for compressor blades operating under highly negative incidence angle which is typical during engine groundstarts or windmilling relights. Although this is a very frequently occurring situation during the life of an aero engine, turbomachinery components are rarely tested under those conditions in the sake of resource saving. However, performance engineers require some knowledge of generic blade loss coefficients under those conditions for the preliminary estimation of the groundstart or relight capability of the engine which is also linked to design decisions such as the volume of the combustion chamber.

A blade element concept is employed to break a 3D compressor blade design down to a number of 2D cross sections and study them separately using a CFD derived 2D blade loss coefficient database. Several different ways to synthesize the 3D blade out of the 2D sections are herein presented based on different expressions of blade aerodynamic coefficients. An investigation based on the expressions of the aerodynamic coefficients is conducted in order to justify the applicability of the blade element theory at such off-design conditions. The most suitable parameter set to represent a three dimensional blade design by a number of radially stacked two dimensional profiles is identified.

The analysis shows that the approach based on pressure change and tangential force coefficients can more adequately approximate the performance of the 3D blade and therefore can be safely employed for a preliminary off-design blade performance studies.

NOMENCLATURE

α_m	Mean flow angle $\tan\alpha_m = 0.5(\tan\alpha_1 + \tan\alpha_2)$
C_L	Lift coefficient
C_D	Drag coefficient
C_p	Pressure rise coefficient
C_f	Tangential force coefficient
c_x	Axial velocity
c_m	Mean velocity $c_x/\cos\alpha_m$
D	Drag force
h	Blade chord
L	Lift force
P_{tot}	Total pressure
P_{st}	Static pressure
R^2	R-square estimator $\frac{\sum(\widehat{y_i}-\bar{y})^2}{\sum(y_i-\bar{y})^2}$
SSE	Sum of Squares Due to Error $\sum(y_i - \widehat{y_i})^2$

s	Blade spacing
X	Axial force on the blade
Y	Tangential force on the blade
α	Flow angle relative to axial
ρ	Density
$\widehat{y_i}$	Estimator of parameter y_i
$\bar{y}$	Mean value of parameter y
$\overline{\omega}$	Total pressure loss coefficient $\frac{(P_{tot,1}-P_{tot,2})}{(P_{tot,1}-P_{st,1})}$

Subscripts

1, 2	Blade inlet, outlet
x	Axial
m	Mean

INTRODUCTION

Sub-idle is a very crucial operating region for a gas turbine engine as unsuccessful recovery after an eventual flame-out may jeopardise engine, aircraft and passenger's safety. Moreover, recent trends in engine design such as the continuously decreasing core sizes or the fact that most of the modern civil aircrafts are powered by only two engines rather than four, make meeting the certification requirements for the relight process as set by the main certification bodies (FAA, EASA) an extremely challenging task. The challenge becomes even greater if it is taken into account that the ratio of the required windmilling offtake power upon core engine size is gradually increasing and that modern combustor design is definitely oriented towards lower emission configurations at expense of the relight capability.

Therefore, the engine properties defining its relight performance, such as windmilling drag, core and by-pass airflows, shaft rotational speeds, flame-out core engine component losses, pull-away duration time etc., must be known prior to finalisation of the engine cycle, size and ratings to ensure a satisfactory engine response under emergency conditions but also because they strongly affect the aircraft design in terms of the size of the vertical tail, the wing, the pylon and the landing gear system [1]. In addition, windmill data is also important for the certification of an engine for extended engine-out operation over water which is more specifically influenced by the windmilling performance under icing or even locked rotor conditions. Finally, the significance of the secondary power extraction capability for accessories design or the estimated pressures and temperatures for combustor or exhaust nozzle detailed design must be underlined. The latter justify the need of reliability in the engine simulation techniques used for the prediction of the above mentioned phenomena, the so-called sub-idle engine models.

In general, there are two major categories of sub-idle models; complete aerothermo cycle models and component specific, loss coefficient based models. The former can be defined as a typical transient engine performance model with component characteristics towards very low speed regimes. Derivation of those characteristics can be achieved using pure mathematical techniques such as map extrapolation, empirical equations to account for the low speed physical phenomena or combination of the two methods. In general, they are similar to the above-idle models, based on thermodynamic calculations and component matching techniques and are used to predict the transient operating lines of an engine during start-up processes. Several attempts to predict windmilling characteristics of turbojet or turbofan engines have been reported within the literature [2] [3]. However, the lack of experimental data as well as the complexity and the low level of understanding of the phenomena occurring within the engine at low power settings do not allow any of those approaches to offer a high level of reliability.

For this reason more research on component losses was carried out and set the base for the development of mainly analytical techniques for the prediction of the major windmilling engine characteristics such as air flow, drag and shaft rotational speeds. Several experimental tests conducted by NACA in 50's attempted to address the issues of a windmilling engine [4] [5] [6] [7]. In addition, Lefebvre commented on the relighting performance of an engine from the combustion's point of view [8]. Work on the empirical interpretation of large engine data for air flow and internal drag predictions has been presented by ESDU [9], while low speed rig tests are strongly recommended by Kurzke for the better understanding of the sub-idle phenomena [10] [11]. Alternative representation of component characteristics has been suggested by a number of authors [2] [10] [11] [12] [13]. According to them the isentropic efficiency map is replaced by a specific torque map. In this way the discontinuities of the efficiency definition at low speeds can be totally avoided. A detailed procedure for sub-idle map generation in several different formats as well as theoretical background on map generation is given in [14].

Undoubtedly, compressor is the component where phenomena of high complexity take place. A significant amount of effort has been put on understanding the low speed compressor aerodynamics and enhancing the physical background of the performance prediction methods [15]. At very low shaft rotational speeds the blade operation is dominated by highly negative incidences mainly occurring at the stators while rotors are operating at relatively less negative incidences but still at negative values (typical locked rotor incidence values are in the order of -60 deg depending on the blade inlet angle design) [16]. The latter implies massive energy losses through the blade channel. The most extreme boundary of compressor or turbine sub-idle operation is the locked-rotor condition which occurs when the ram air has not enough momentum to cause free shaft rotation, thus rotor blade rows are locked throughout the engine [17]. Essentially, the flow at that regime is incompressible as the inlet Mach number is never higher than 0.3, thus incompressible flow theory is applicable. In previous studies conducted on turbofan engines, the off-design compressor performance models proposed by Howell [18], Griepentrog [19] or Horlock [20] have been used. In other cases, assumptions are made in order an approximate windmill compressor characteristic to be defined, before its use in a theoretical calculation for turbojet engines [21]. One of the most recent studies on windmilling compression systems conducted by Prasad et al. [22], explains in great detail the windmilling behaviour of a large turbofan engine based on numerical simulations of the fan stage revealing some of the dynamics of the recirculation region onto the blades.

The success of an engine relight and pull away process simulation relies at a great extent upon the component modelling introduced into it. Nevertheless, a generic model for the prediction of such off design compressor operation cannot be easily found within the literature as most of the traditional, predictive modelling is focused around the design point operation. Additionally, it can be easily realised that the massive recirculation regions at low speeds cannot be described by these models. Thus, the research on the derivation of novel windmilling models is a vital factor which the engine performance prediction solvers will have great benefit from as prediction of compressor characteristics with greater accuracy would be feasible. Moreover, the enhancements on the compressor loss modelling imply a better estimation on the windmilling losses of the bypass duct of the engine due to the presence of the OGV's which operate at off-design as well. As a consequence windmilling internal drag predictions become also more accurate.

In this paper, a modelling approach for compressors operating at highly negative incidence angles is proposed. A database of 2D blade profiles is employed for the generation of the 3D blade out of 2D sections by stacking them radially using a blade element approach. The database essentially consists of pressure loss and deviation values derived by 2D numerical simulations of a compressor cascade at different solidities and incidence angles with always the same aerofoil profile. A comparison between the initial 3D blade and the one derived out of the stacked 2D cross sections is conducted in terms of overall blade loss. The comparison is based on the expressions of the blade aerodynamic coefficients. The objective is to verify whether a three dimensional blade design can be sufficiently represented with a number of radially stacked two dimensional profiles in terms of its overall performance.

COMPRESSOR PERFORMANCE AT HIGHLY NEGATIVE INCIDENCE

Fundamentally, the blade element theory suggests that each 3D blade consists of infinite 2D cross sections along its span, assuming that each such element operates as a 2D aerofoil without any interaction with the rest. Thus, the 3D blade can be designed by stacking radially a certain number of 2D blade elements of known performance. Deep mathematical analyses based on that concept can be found in [23] and [24] while a very enriched list of references can be also found in [25].

The question is whether such an analysis could be valid for typical windmilling conditions, that is extremely far off the blade design region. For the latter to be verified, any kind of 3D compressor blade design could be approximated by a number of 2D sections also at off-design conditions. Therefore, having a number of systematic, 2D cascade data for different incidences, solidities, stagger and camber angles, will allow the performance prediction of any 3D blade design by just putting together the 2D profiles. This simplification must be done with awareness though, as all the 3-dimensional effects caused by secondary radial flows are not taken into account.

In order to prove the applicability of the above explained concept on compressor cascades at highly negative incidence, a comparative study to verify whether a 3D blade performance can be approximated by a number of radially stacked 2D sections was undertaken. To do so, the flowfield patterns at specific spanwise positions obtained with a 3D annular cascade CFD simulation approach have been compared against stand alone 2D simulations with exactly the same features (solidity, incidence and stagger angle) as the correspondent radial position of the 3D blade. The locations have been chosen at three radii: at 10% and 90% in the spanwise direction, in order to minimize the wall effects, and at mid-span position (50%). The blade performance evaluation in each case was carried out on the basis of the lift, drag, pressure change and tangential force coefficients knowingly that the effect of all the radial flows that may occur in the three dimensional channel will not be taken into account by the 2D simulations.

Numerical models

The commercial flow prediction package CFX has been used for all the simulations described herein. As it is extremely challenging for CFD to capture separated flows, the solver was initially calibrated against in-house experimental data from a compressor cascade at highly negative incidence. Details of this work have been described in a previous paper [16]. This process allowed more confident use of the numerical tool.

The flow comes axially towards the blade thus the flow incidence equals to the blade inlet angle which in this case is -58 deg at mid-span varying within a range of $\pm 7\%$ between the hub and the tip of the blade (Fig. 1). The inlet flow angle is always zero and constant for all the cases, in order to achieve the desired negative incidence value of -58 deg at mid-span.

As far as the computational mesh is concerned, an O-mesh hexaedric mesh configuration has been employed for the treatment of the region around the blade. The total number of hexaedra elements is approximately 1.2 million cells after a grid de-

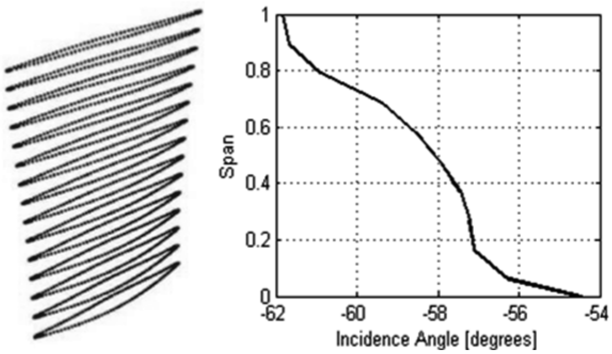

Figure 1. Three dimensional blade spanwise incidence distribution.

pendency study. Extra care has been taken for the tuning of the mesh parameters to ensure faster convergence, thus the 3x3x3 determinant of the elements has been kept between 0.5 and 1 and the skewness of all elements is more than 20 deg. In addition, a careful balance between the element aspect ratio and the near wall y^+ was conducted. More specifically, the y^+ near the wall has been kept below 2 with not less than ten cells into the boundary layer region, wherever the aspect ratio of the cells allowed it, whereas an automatic switch to wall functions initiated by the solvers takes place in all cases that cell aspect ratio does not allow for the desired near wall y^+ value to be achieved. Regarding the turbulence closure of the problem, a k-ω - SST model has been chosen after an extensive parametric analysis as explained in [16]. Finally, a total pressure inlet coupled with a mass flow outlet boundary condition employed for all the simulations. A meridional view of the three dimensional domain is shown in Fig. 2.

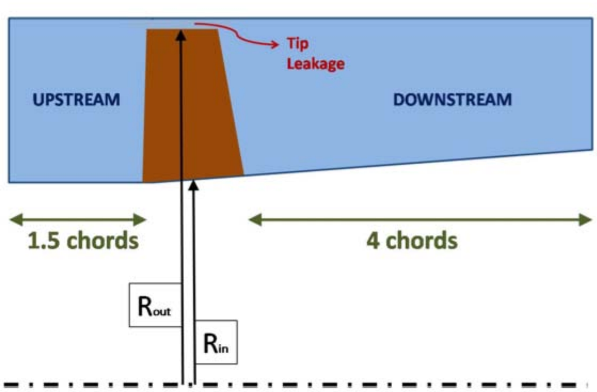

Figure 2. Meridional plane of the three dimensional domain used for the 3D simulations.

The two dimensional profile models have been also developed with a similar to the 3D solver set-up in order for the above mentioned blade element based flow comparison to be carried out.

The simulations were conducted for inlet Mach number 0.1 in all cases. This makes both total pressure loss coefficient and flow exit angle independent upon this parameter as the flow is kept incompressible. Additionally, the Reynolds number is above $2 \cdot 10^5$ thus the previously mentioned properties are also independent upon it [25]. The calculation of the properties of interest has been made at two blade chords downstream to allow for better flow mixing. Mainly, the choice is related with the entropy generation rate and the occurrence of mixing losses as we go further downstream of the blade trailing edge. In other words, the more space is given to the flow to expand, a higher percentage of its dynamic head is transformed into pressure loss, until all the losses of the system will be developed, theoretically in infinite distance downstream. In most cases the majority of the loss needs no more than one blade chord downstream space to appear. However, at off-design cases, such the one studied herein, more space is required until the flow is fully mixed. This happens because the recirculating areas cause a significant blockage to the channel and thus the flow accelerates until the exit, where the flow effective area starts gradually increasing again. This implies a static pressure recovery that continues for a few chord lengths downstream until wakes are fully mixed. This also affects the total pressure loss coefficient that demonstrates strong dependency upon the downstream position due to the big static pressure changes as shown in Fig. 3. Therefore, it is calculated at approximately two chords downstream where the flow is totally mixed up and all the losses have appeared [26] [27] [28] [29].

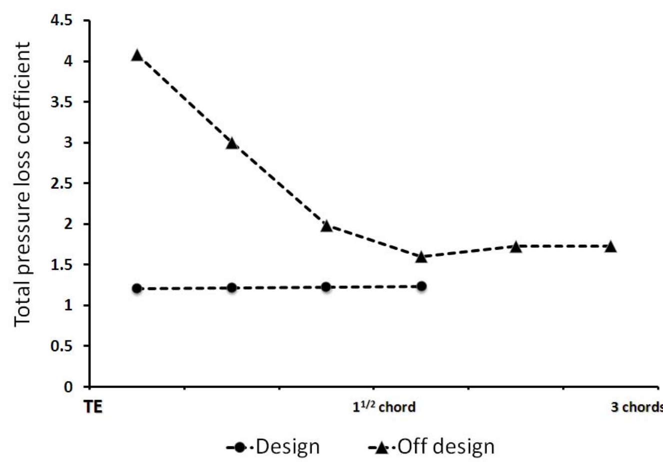

Figure 3. Total pressure loss coefficient as a function of the axial distance from trailing edge at design and highly negative incidence conditions.

RESULTS AND DISCUSSION

Fundamentally, blade performance is represented by non-dimensional aerodynamic coefficients in respect to the lift and drag forces (C_D, C_L), the tangential force (C_f) and the static pressure change along the channel (C_p). Those properties are defined as:

$$C_D = \frac{D}{\frac{1}{2}\rho c_m^2 h} \tag{1}$$

$$C_L = \frac{L}{\frac{1}{2}\rho c_m^2 h} \tag{2}$$

$$C_f = \frac{Y}{\frac{1}{2}\rho c_x^2 s} \tag{3}$$

$$C_p = \frac{p_2 - p_1}{\frac{1}{2}\rho \overline{c_x}^2} = \frac{X}{\frac{1}{2}\rho \overline{c_x}^2 s} \tag{4}$$

The forces on which the above coefficients are based are shown in the Fig. 4.

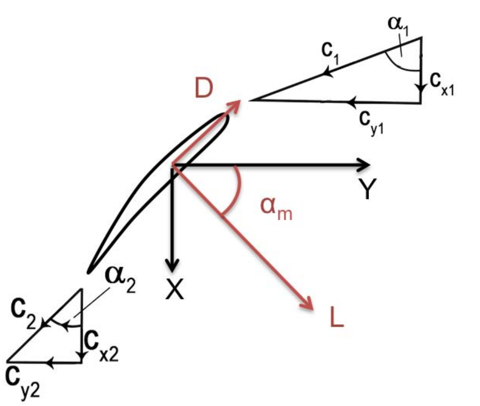

Figure 4. Lift (L), drag (D), static pressure change (X) and tangential (Y) forces as exerted by a cascade blade upon the fluid at design conditions [25]. At highly negative incidence conditions these forces exerted by the fluid upon the blade.

An alternative expression of those coefficients can be derived using the total pressure loss coefficient as well as the inlet and outlet flow angles (α_1 and α_2).

$$C_L = 2\frac{s}{h}\cos\alpha_m(\tan\alpha_1 - \tan\alpha_2) - C_D \tan\alpha_m \tag{5}$$

$$C_D = \overline{\omega}\frac{s}{h}\cos^3\alpha_m \tag{6}$$

$$C_f = 2(\tan\alpha_1 - \tan\alpha_2) \tag{7}$$

$$C_p = C_f \tan\alpha_m - \overline{\omega} \tag{8}$$

Two different approaches are used for the calculation of the overall blade performance; the first one relies on the calculation of C_f and C_p coefficients based on the observed flow exit angle and static pressure drop respectively. The total pressure loss coefficient is then calculated using Eq. 8. In the second approach, the total pressure loss coefficient as calculated internally by the CFD solver and the flow exit angle are used for the calculation of C_D and finally C_L. The qualitative difference between the two approaches is that the first one correlates the aerodynamic coefficients directly with the flow properties such as flow angles and losses and not with their resulting forces on the blade as the second one set does.

The results from the 3D and the 2D simulations are hereafter compared using the previously described approaches. Starting from the comparison of the outlet flow angle (α_2) which primarily defines the tangential force coefficient (C_f), it can be seen that the maximum difference between the full 3D and the 2D profile simulations at the corresponding positions, is in the order of 11% at the hub with the fully 3D simulation to predict slightly reduced value. The latter has an impact on the calculation of the tangential force coefficient (see Fig. 6) where the maximum difference between the two approaches (3D and quasi-3D) is of an order of 12% for the mid-span position and not at the hub as expected. This simply happens because the percentage error of the tangent of the exit flow angle obtains its maximum value at the mid-span (19.1%).

In addition, the static pressure drop across the passage defines the static pressure drop coefficient (C_p) and the comparison between the 2D and 3D cases is even more encouraging as the maximum error is not more than 7% for the hub position, as illustrated in Fig. 7. For its calculation, the average axial velocity between the upstream and downstream position has been used as the difference between the two is too significant to be neglected.

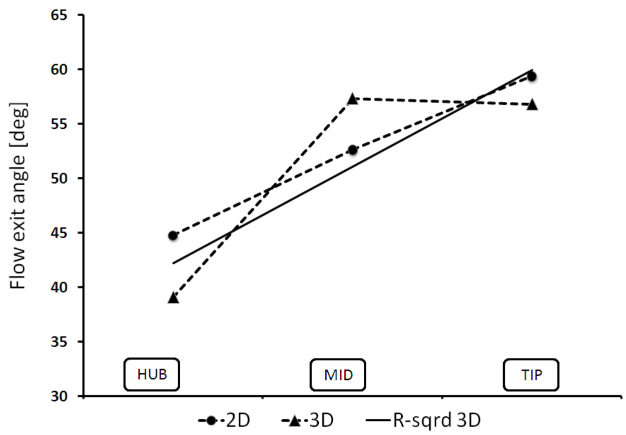

Figure 5. Flow exit angle distribution.

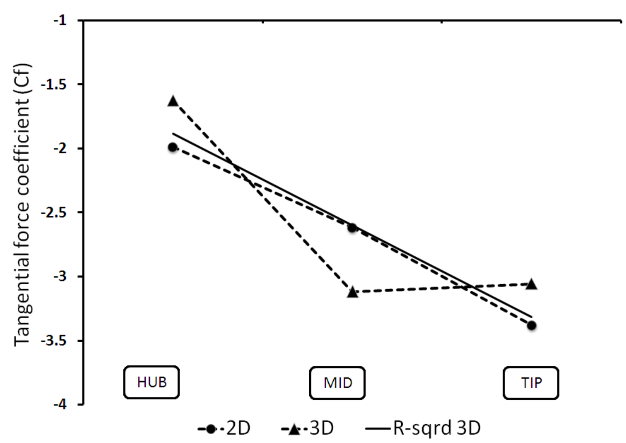

Figure 6. Tangential force coefficient distribution.

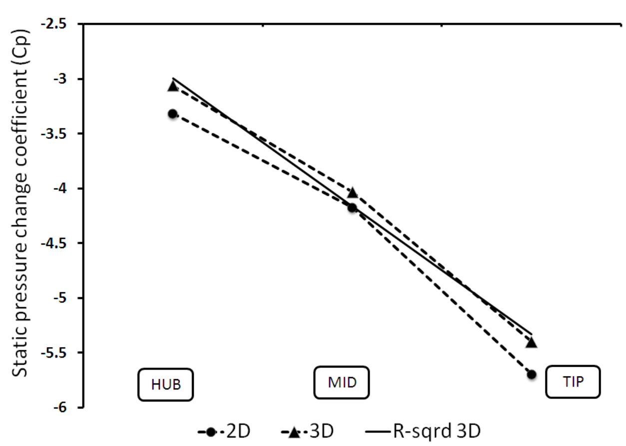

Figure 7. Static pressure change coefficient distribution.

Having obtained those non-dimensional coefficients the total pressure loss coefficient can be calculated by Eq. 8. The calculated values at every position are illustrated in Fig. 8. This comparison reveals the maximum error at the mid-span position in the order of 35%, mainly due to the error coming from the tangential force coefficient calculation. The observed error at the two other positions (hub and tip) is not more than 7%.

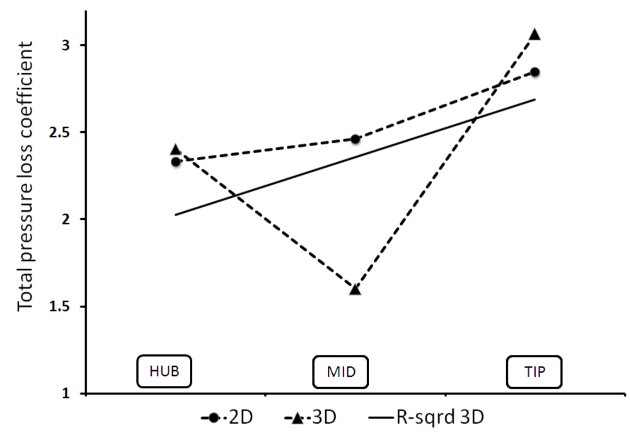

Figure 8. Analytically calculated total pressure loss coefficient.

On the other hand, if the total pressure loss (as directly predicted by the solver - see Fig. 9) and flow deviation are used for the derivation of the C_D and C_L coefficients, the plots in Figs. 10 and 11 are obtained.

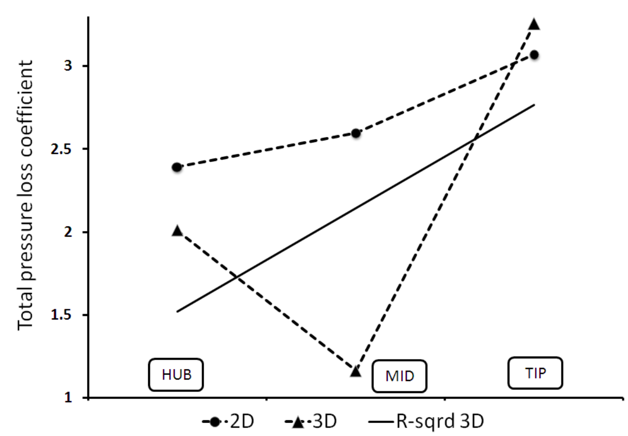

Figure 9. Total pressure loss coefficient as predicted by the CFD solver.

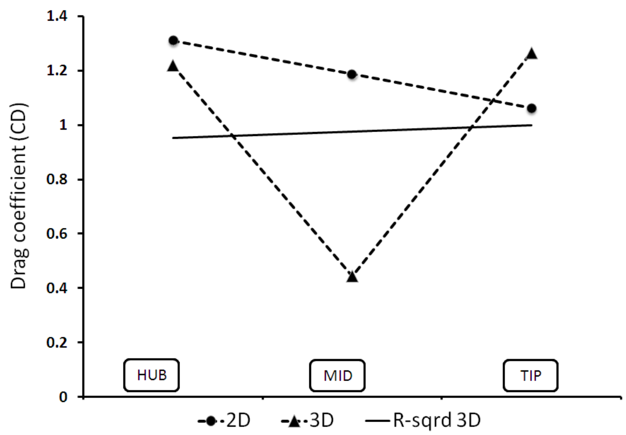

Figure 10. Drag coefficient distribution.

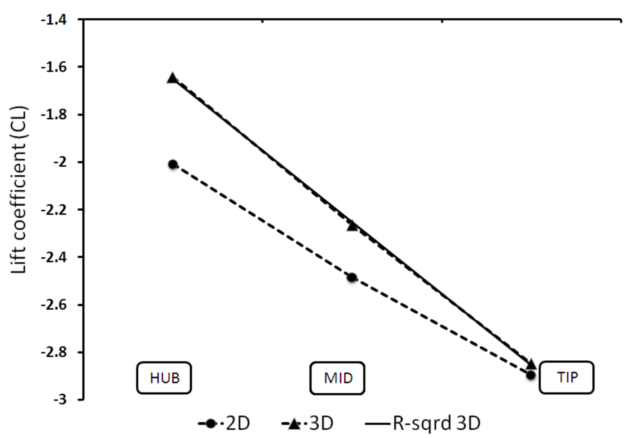

Figure 11. Lift coefficient distribution.

By looking at Figs. 10 and 11 and comparing the 3D against the 2D case, it can be easily observed that the large deviation at the predicted total pressure loss coefficient previously underlined, is directly reflected on the drag coefficient thus affects the lift coefficient as well. The maximum error appears at the mid-span position. A significant amount of error (18%) appears also in the lift coefficient calculation. Finally, the comparison between Figs. 8 and 9 reveals that for the 3D blade simulation the solver predicted values are lower than the calculated by the C_p and C_f coefficients by a maximum of 28%, confirming that the numerical tool tends to under-estimate the total pressure loss [30]. On the other hand, there is no significant error between the calculated and predicted values regarding the 2D profiles as apparently the flow structures are simpler and thus more easily predicted by a numerical simulation. In general, there is always a noticeable difference between the 2D and 3D results. This is expected in the sense that all the flow patterns developed in the 3D case such as endwall losses or radial flows due to the 3D blade shape do not exist in the 2D simulations and therefore are neglected. However, the regression analysis presented in the next section reveals that the 3D flow effects have no vital impact in the calculation of the overall blade performance using the pressure rise and tangential force coefficients.

Regression analysis

The suitability of the aerodynamic coefficient expressions to describe extreme partload blade operation is investigated by a regression analysis on the above presented data sets. In all cases a first degree polynomial fit is employed to describe the three dimensional blade data as shown in Figs. 5 to 11. In such kind of analysis the fit goodness is assessed using the Summed Square Due to Error (SSE) as well as the R-square indices, defined as:

$$SSE = \sum (y_i - \widehat{y}_i)^2 \tag{9}$$

$$R^2 = \frac{\sum (\widehat{y}_i - \overline{y})^2}{\sum (y_i - \overline{y})^2} \tag{10}$$

It is reminded that an SSE value closer to 0 as well as R-square values closer to 1 indicate a better fit. More details about fit goodness estimators can be found in [31].

Figure 12 shows the fit goodness estimators for the blade coefficients as defined above. It can be seen that the achieved fitting in the first set of parameters (C_p and C_f expressions) is definitely better than the linear approximation of the C_D, C_L based expressions. More specifically, the linear approximation of the flow exit angle, tangential force and static pressure change coefficient is quite successful as the SSE is kept at low levels while the R-squared parameter gets values very close to unity. Nevertheless, poor fitting on the calculated values of the total pressure loss coefficient can be observed which, however, is not as poor as the fitting on the predicted by the solver total pressure loss coefficient. In addition, the linear approximation does not look very promising as far as the drag coefficient is concerned due to the large errors propagated in its expression by the total pressure loss coefficient prediction and the cubic dependency upon the flow exit angle (see Eq. 6). Finally, the regression estimators obtain quite satisfactory values regarding the lift coefficient approximation, but by no means this confidence is comparable with the reliability offered by the first parameter set. Therefore, the above analysis showed that a linear approximation of off-design blade performance data is much more worthy to be done in terms of tangential force and static pressure change coefficient as there is high confidence on this kind of estimation.

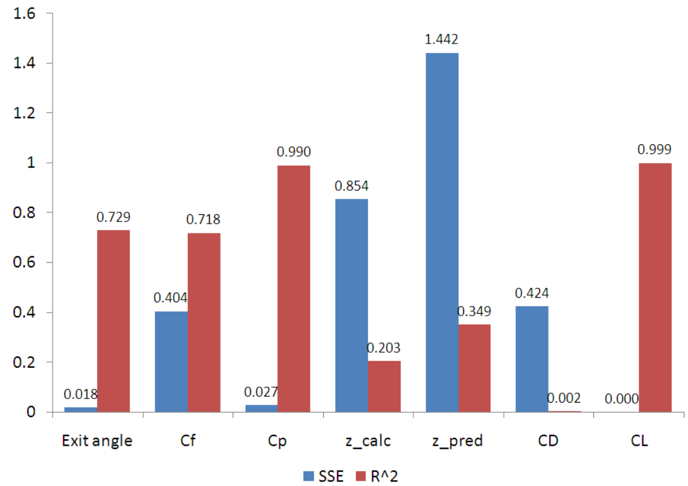

Figure 12. Regression evaluation factors for the linear fit on the three dimensional blade data.

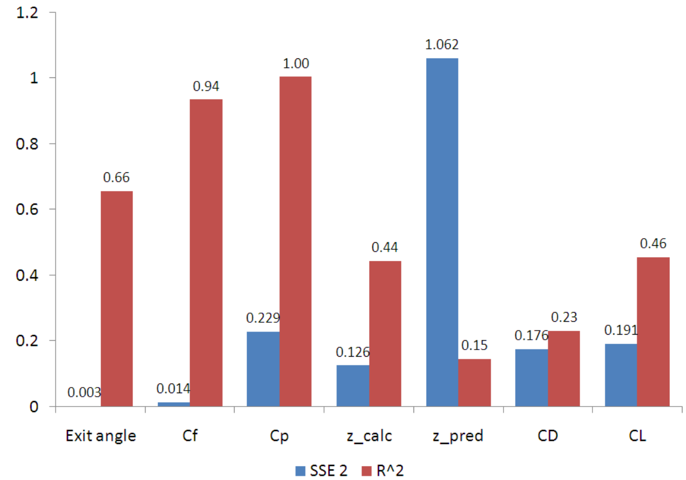

Figure 13. Evaluation factors for the prediction of the three dimensional regression fits using blade element data.

Attempting now to take advantage of the above concluded statement, a comparison between the linear regression fits and the blade element result is conducted. Similar to the above indices are used to evaluate how well the two dimensional data are able to predict the regression lines previously fit in the three dimensional blade data. In other words, for this second comparison, the blade element results are considered as the estimators of the regression lines. The fit goodness is evaluated in a similar approach. As shown in Fig. 13, the approach based on the C_p and C_f expressions offers high reliability as a minimum SSE are combined with very high R-squared values which in fact proves the suitability of the blade element derived coefficients for the approximation of the three dimensional regression line. Relatively high confidence is also observed for the total pressure loss coefficient approximation. On the other hand, the poor prediction of the solver derived total pressure loss coefficient value, leads to an equally poor approximation of the drag coefficient while a marginally accepted lift coefficient prediction is also observed. In general it has been shown that the blade element data are able to predict the three dimensional blade performance as long as the tangential force and static pressure change coefficients are employed.

The two-step regression analysis presented above justified the suitability of the blade element tangential force and pressure change coefficient to predict the performance of the three dimensional blade at high level of confidence. Initially, it has been shown that the three dimensional blade data can be better represented by the previously mentioned set of coefficients, revealed by the regression goodness factors. The latter implies a lower error in the estimation of the aerodynamic performance of the 3D blade after a spanwise integration. In addition, as the results showed, the C_p and C_f two dimensional data match better the regression line of the three dimensional simulations, while this does not happen when the second parameter set is used. From these observations, it is understood that a whole blade performance estimation, based on two dimensional blade element data expressed in terms of tangential force and pressure change coefficient, demonstrates better applicability than the analysis based on the lift and drag coefficient definitions.

This is partially justified by the considerations on the numerical solver's capability to predict the amount of loss that a flow experiences through turbomachinery passages. It is well established that CFD solvers are in general reliable enough at predicting static pressure drop (thus kinetic energy increase) due to flow acceleration as in this case that despite the diverging channel the flow experiences an acceleration due to the negative incidence effects. However, their predictive capability is crucially lower when they reach the point that the dissipation of kinetic energy into energy loss must be defined, as there is lack of predictability as far as the entropy increase mechanisms of the flow are concerned [32] [33]. As a result, the static pressure decrease in such flows can be well predicted, but the prediction of the total pressure (energy) loss is generally poor. On the other hand, flow deviation is not heavily affected by the weakness to predict the velocity profile at the exit as this property reflects just the direction of the velocity vectors (and not their magnitude) which is primarily affected by the channel and the size of the circulation area rather than the actual magnitude of the outlet flow. The two latter points provide the advantage to the C_p and C_f epxressions against the C_D and C_L coefficients. The former parameter set is based on static pressure loss and deviation predictions while this is not the case for the latter which relies exclusively on total pressure loss prediction. In addition, the mathematical calculation of C_D and C_L is more complicated and more dependent on the total pressure loss than the simpler and more explicit definition of C_p and C_f coefficients. As a result, the errors in the prediction of all the properties have a stronger impact on the drag and lift coefficients.

It can be argued here that no certain comparison can be done between the 2D and 3D cases as far as the total pressure loss is concerned due to the radial flows occurring in the 3D case increasing significantly the overall amount of energy loss. However, as can be seen from the above results it does not look that 3D flows have a strong impact in the average loss. 3D flow structures might rearrange radially the flow layers (and this justifies the difference between the 2D and 3D property distribution) but no significant increase in the overall loss occurs as a large percentage of the total pressure loss (and probably of a bigger order of magnitude than the radial losses) comes from the separated regions along the span. Hence, the performance of the individual 2D profiles can easily be taken from a database, thus no complicated three dimensional blade loss studies are required at a first approximation such as the preliminary engine off-design estimation phase.

Consequently, a simplified blade element theory looks to be valid also for far off-design cases as long as a suitable definition of the aerodynamic blade coefficients is employed. This finding allows the approximate performance estimation of every 3D blade operating under such off-design conditions using a radially stacked number of 2D profiles.

The whole engine modelling perspective

The above presented approach can significantly enhance the whole engine performance predictive capability, thus the concept of the *advanced performance simulation* is being pushed forward. As explained in [34] and [35], the coupling between a performance solver and component models of higher fidelity can improve the overall accuracy of an engine performance solver. In this context, an insight into the sub-idle compressor behaviour, such as the one present herein, allows for the more successful representation of its low speed characteristics, which are of vital importance for the accurate simulation of starting and relighting manoeuvres.

Up to the moment, most of the compressor map generation techniques are based on the extrapolation of the above idle area towards the sub-idle. However, lack of physical background prevents those methods from providing accurate component characteristics. More detailed research within the low speed regime of operation is highly required. As illustrated in [14], map representation in terms of *torque* as well as a definition of the zero speed curve are key aspects for engine modelling of higher fidelity as interpolation of the characteristic between zero and above idle will be feasible. Moreover, employment of the torque parameter, instead of the conventional efficiency factor, allows for successful modelling at operating points where the latter reaches infinite values. Consequently, a generic approach for compressor zero speed line prediction is more than necessary, and this is where the current technique has a great contribution. In other words, a blade element loss and deviation database can be employed for the stacking of a 3 dimensional blade design, which in turn, is introduced within a suitable stage stacking technique [14] or even a throughflow analysis, for the whole compressor zero-speed line definition.

Additionally, engine internal drag estimation can be also conducted in great accuracy. As described in [9], the fan OGV's are the major source of engine internal drag under windmilling conditions as most of the mass flow prefers to pass through the bypass duct instead of the core engine. Due to the very low windmilling fan rotational speed, the OGV's operate at highly negative incidence imposing a great amount of losses in the air stream. It is clear that internal drag predictions and studies can be performed using a blade element database allowing for an early estimation of the windmilling performance characteristics of the engine, improving the off-design understanding of the product even from the early design phases of it.

CONCLUSIONS

A modelling approach for compressors operating at highly negative incidence angles is proposed in this work. More specifically, a decomposition of a 3D blade into 2D cross sections (blade elements) has been carried out. Numerical simulations in both configurations were conducted at incompressible flow conditions and at highly negative incidences (-58 deg) in order to verify whether the three dimensional blade design can be approximated by a radial stacking of the two dimensional profiles.

The main conclusions can be summarised in the following bullet points:

- In overall, the analysis has shown that the performance of a three dimensional blade operating at highly negative incidence can be estimated by the spanwise integration of blade element performance data expressed in terms of *tangential force* and *pressure change* coefficient.
- The tangential force and pressure change coefficient definitions require no total energy loss or blade forces to be predicted but only static pressure change and deviation angle. Hence, the impact of the flow solver's weakness to predict pressure losses on the definition of blade performance is partially avoided as the overall losses can be now mathematically estimated from Eq. 8.
- The regression analysis suggests that the linear approximation of such off-design blade performance data using the tangential force and static pressure change coefficients offers a higher level of confidence.
- Stacking the blade element data in respect to the tangential force and static pressure change coefficients allows for an

accurate prediction of the regression lines of the 3D blade.

• The error in the performance prediction of the three dimensional blade by a spanwise integration of the blade element data is directly proportional to the regression errors generated by the approximation of the 3D data with their linear fits and the estimation of the linear using blade element simulations. Therefore, it can be concluded that the C_p and C_f based integration offers higher predictive accuracy when the two dimensional profiles are radially stacked to represent the three dimensional design.

• The above presented approach enhances the part speed compressor blade modelling offering also further benefits to the whole engine performance prediction capability; OGV and by-pass duct modelling can be improved allowing for a preliminary estimation of the engine windmilling characteristics such as the internal drag, core and bypass duct mass flow or shaft rotational speeds even from the early design phases of it.

ACKNOWLEDGMENT

The authors would like to express their gratitude to Stephen Brown, Richard Tunstall and Arthur Rowe from Rolls-Royce plc. for their support to this project.

REFERENCES

[1] Anderson, B. A., Messih, D., and Plybon, R. C. "Engine-out performance characteristics". *ISABE 97-7216*.

[2] Riegler, C., Bauer, M., and Schulte, H., 2003. "Validation of a mixed flow turbofan performance model in the sub-idle operating range". *ASME Turbo Expo, Atlanta, Georgia, USA*.

[3] Gaudet, S. R., and Gauthier, J. E. D., 2007. "A simple sub-idle component map extrapolation method". *ASME Turbo Expo, Montreal, Canada*.

[4] Hatch, J., 1958. "Comparison of experimentally and analytically determined windmilling characteristics of a compressor with low over-all pressure ratio". *NACA*(RM E57L12a).

[5] Vincent, K. R., Huntley, S. C., and Wilsted, H. D., 1952. "Comparison of locked-rotor and windmilling drag characteristics of an axial-flow-compressor turbo-jet engine". *NACA RM-E51K15*.

[6] Sobolewski, A. E., and Farley, J. M., 1951. "Steady-state engine windmilling and engine speed decay characteristics of an axial-flow turbojet engine". *NACA RM-E51I06*.

[7] Wallner, L. E., and Welna, H. J., 1951. "Generalization of turbojet and turbine-propeller engine performance in windmilling condition". *NACA RM-E51J23*.

[8] Lefebvre, A. H., 1923. Theoretical aspects of aero-engine altitude relighting performance. Tech. rep., Cranfield, College of Aeronautics.

[9] ESDU, 1984. Estimation of windmill drag and airflow of turbo-jet and turo-fan engines. Tech. Rep. 81009.

[10] Kurzke, J., 1996. "How to get component maps for aircraft gas turbine performance simulations". *International Gas Turbine and Aeroengine Congress and Exhibition, Birmingham, UK, 1996*.

[11] Riegler, C., Bauer, M., and Kurzke, J., 2000. "Some aspects of modeling compressor behavior in gas turbine performance calculations". *ASME Turbo Expo, Munich, Germany, 2000*.

[12] Jones, G., Pilidis, P., and Curnock, B., 2001. "Compressor characteristics in gas turbine performance modelling". *ASME Turbo Expo, New Orleans, Louisiana*.

[13] Jones, G., Pilidis, P., and Curnock, B., 2002. "Extrapolation of compressor characteristics to the low-speed region for sub-idle performance modelling". *ASME Turbo Expo, Amsterdam, The Netherlands*.

[14] Zachos, P. K., Aslanidou, I., Pachidis, V., and Singh, R., 2011. "A physically enhanced method for sub-idle compressor map generation". *Journal of Engineering for Gas Turbines and Power,* **133**.

[15] Pollard, D., and Gostelow, J. P., 1967. "Some experiments at low speed on compressor cascades". *Journal of Engineering for Power,* **89**(3), pp. 427–436.

[16] Zachos, P. K., Pachidis, V., Charnley, B., and Pilidis, P., 2009. "Flowfield investigation of a compressor cascade at high incidence - part 1: Pneumatic probe measurements". *ASME Turbo Expo, Orlando, USA*.

[17] Walsh, P. P., and Fletcher, P., 1996. *Gas Turbine Performance*, 2nd ed. Blackwell Publishing.

[18] Howell, A. R., 1945. "Design of axial compressors". *Proceedings of IMechE,* **153**, p. 452.

[19] Wallis, R. A., 1983. *Axial flow fans and ducts*. John Wiley & Sons.

[20] Horlock, J. H., 1973. *Axial flow compressors. Fluid mechanics and thermodynamics*. Robert Krieger publishing company, New York.

[21] Shou, Z. Q., 1981. "Calculation of windmilling characteristics of turbojet engines". *ASME Journal of Engineering for Power,* **103**(1), pp. 1–12.

[22] Prasad, D., and Lord, W. K., 2010. "Internal losses and flow behavior of a turbofan stage at windmill". *Journal of Turbomachinery,* **132**(3).

[23] Robbins, W. H., Jackson, R. J., and Lieblein, S., 1965. "Blade element flow in annular cascades". *NASA SP-36, Chapter VII*.

[24] Lieblein, S., 1954. Review of high-performance axial flow compressor blade element theory. Tech. Rep. RM E53L22, NACA.

[25] Dixon, S. L., 2005. *Fluid mechanics and thermodynamics of turbomachinery*, 5th ed. Pergamon Press.

[26] Cumpsty, N. A., and Horlock, J. H., 2006. "Averaging

nonuniform flow for a purpose". *Journal of Turbomachinery,* **128**, pp. 120–129.
[27] Cumpsty, N. A., 1989. *Compressor aerodynamics*. Longman Scientific and Technical.
[28] Prasad, A., 2005. "Calculation of the mixed-out state in turbomachine flows". *Journal of Turbomachinery,* **127**, pp. 564–572.
[29] Gostelow, J. P., 1984. *Cascade aerodynamics*. Pergamon Press.
[30] *ANSYS CFX Manual*.
[31] Maindonald, J. H., 2010. *Data analysis and graphics using R: an example-based approach*. Cambridge University Press.
[32] Denton, J. D., 1993. "Loss mechanisms in turbomachines". *IGTI scholar lecture*.
[33] Denton, J. D., 2010. "Some limitations of turbomachinery cfd". *ASME Turbo Expo, Glasgow, Scotland, UK*.
[34] Templalexis, I., Pilidis, P., Pachidis, V., and Kotsiopoulos, P., 2006. "Development of a two dimensional stremaline curvature code". *Journal of Turbomachinery*.
[35] Pachidis, V., Pilidis, P., Talhouarn, F., Kalfas, A., and Templalexis, I., 2006. "A fully integrated approach to component zooming using computational fluid dynamics". *ASME Journal of Engineering for Gas Turbines and Power,* **128**.